A quasi-realtime x-ray microtomography system at the Advanced Photon Source

Yuxin Wang[a], Francesco De Carlo[a], Ian Foster[b], Joseph Insley[b],
Carl Kesselman[c], Peter Lane[b], Gregor von Laszewski[b],
Derrick Mancini[a], Ian McNulty[a], Mei-Hui Su[c], Brian Tieman[a]

[a]Advanced Photon Source, Argonne National Laboratory
[b]Mathematics and Computer Science Division, Argonne National Laboratory
[c]Information Sciences Institute, University of Southern California

ABSTRACT

The combination of high-brilliance x-ray sources, fast detector systems, wide-bandwidth networks, and parallel computers can substantially reduce the time required to acquire, reconstruct, and visualize high-resolution three-dimensional tomographic data sets. A quasi-realtime computed x-ray microtomography system has been implemented at the 2-BM beamline at the Advanced Photon Source at Argonne National Laboratory. With this system, a complete tomographic data set can be collected in about 15 minutes. Immediately after each projection is obtained, it is rapidly transferred to the Mathematics and Computing Sciences Division where preprocessing and reconstruction calculations are performed concurrently with the data acquisition by a SGI parallel computer. The reconstruction results, once completed, are transferred to a visualization computer that performs the volume rendering calculations. Rendered images of the reconstructed data are available for viewing back at the beamline experiment station minutes after the data acquisition was complete. The fully pipelined data acquisition and reconstruction system also gives us the option to acquire the tomographic data set in several cycles, initially with coarse then with fine angular steps. At present the projections are acquired with a straight-ray projection imaging scheme using 5-20 keV hard x rays in either phase or amplitude contrast mode at a 1-10 μm resolution. In the future, we expect to increase the resolution of the projections to below 100 nm by using a focused x-ray beam at the 2-ID-B beamline and to reduce the combined acquisition and computation time to the 1 min scale with improvements in the detectors, network links, software pipeline, and computation algorithms.

Keywords: realtime, x-ray microtomography, supercomputing, Globus, HDF, NeXus

1. INTRODUCTION

By providing high-brilliance x-ray beams for crystallography, spectroscopy and microimaging, synchrotron radiation facilities are playing an increasingly important role in research in biological, physical, material, and environmental sciences. Many applications use tomographic imaging to produce a three-dimensional representation of a sample. Using 5-20 keV hard x rays, it is possible to image samples of a few mm thickness at 1 μm resolution in three-dimensions[1–3]; while using soft x rays with a few hundred eV to 2 keV energy, small samples of a few micrometer thickness can be imaged at 50 - 100 nm resolution.[4–6] In principle, the brilliance of third-generation synchrotron radiation facilities allows high-resolution images to be acquired at the rate of tens of images per second if photon statistics were the only concern. This suggests that if a high-speed data acquistion system is implemented to take advantage of the high photon flux, it is possible to acquire enough images for a tomographic data set in a few seconds to a few minutes so that time-resolved observations can be made at few micrometer to tens of nm resolution in three dimensions.

Tomography experiments generate a large amount of data in a relatively short time and demand much computing power for image processing and reconstruction calculations. A high-speed data transfer network and a high-performance computer system are therefore needed to complement the high data acquisition rate to give facility users prompt feedback of the reconstruction results. This is particularly valuable for user-shared facilities where each user has only limited days of operation annually. A quasi-realtime x-ray tomography system has been constructed at the 2-BM (bending magnet) beamline at the Advanced Photon Source (APS) at Argonne National Laboratory. It uses a scintillator-based imaging system to acquire x-ray projections and transfers them to a parallel computer located at the Mathematics and Computer Science Division (MCS) for the preprocessing and reconstruction calculations.

DISCLAIMER

Using this remote computing scheme, the computation time is approximately equal to the acquisition time so that the reconstruction result from the data acquired at the experiment station can be viewed by the operators shortly after the data is acquired.

2. DATA ACQUISITION SYSTEM

The 2-BM beamline was originally constructed for deep x-ray lithography exposure by Lai *et al.*[7] X-ray microtomography experiments were later developed for the beamline by Lee *et al.*[3] The direct projection system shown in Fig. 1 is used to acquire the tomographic projections. The x-ray beam emitted from the bending magnet is monochromatized by a Kohzu double-crystal monochromator then apertured to a 5 mm × 5 mm size. The sample is placed in the apertured beam, and the transmitted x ray illuminates a $CdWO_4$ single-crystal scintillator. The visible light emitted by the scintillator is imaged to a CCD detector by a visible light microscope objective. A 10× objective with numeric aperture of 0.2 is frequently used, but in the current setup, its effective magnification is approximately 5× and its numeric aperture is about 0.1. The scintillator screen is effectively grainless, hence the resolution of the system is determined primarily by the combination of the resolution of the objective and the CCD pixel size. Using the Rayleigh criterion, the resolution of the objective can be estimated to be

$$\delta = 0.61 \times \frac{\lambda}{\text{N.A.}} \approx 0.61 \times \frac{0.5}{0.1} \approx 3\ \mu\text{m}. \tag{1}$$

The CCD has a pixel size of 6.8 μm, correspoonding to roughly a 1.4 μm pixel size at the sample plane. Therefore we estimate the resolution of the images to be about 3 μm (or 2 pixels). This setup approximately satisfies the Nyquist sampling theorem. The resolution can be improved to beyond 1 μm by using a different objective at the cost of a smaller field of view.[3]

The sample's complex index of refraction and the beam propagation distance between the sample and scintillation screen determine whether phase or absorption is the predominant contrast mechanism of the recorded images. Fig. 2 shows one projection of a micromachined gear acquired in phase contrast during a live demonstration of this system at the 1998 SuperComputing Conference. Fig. 3 shows one projection of an ant's head acquired in absorption contrast mode during a recent test.

For each projection, typically 1024×1024 images are acquired in 10 s integration time, or 512×512 images can be acquired in 3 s integration time with 2×2 binning. The CCD data transfer time is about 3 s for 1024×1024 size images and 1 second for 512×512 size images. After each image is acquired, it is saved on a local hard drive, and immediately after the data file is saved, an FTP daemon transfers it to the SGI parallel computer at MCS. A tomographic data set is usually acquired in a few cycles, starting with coarse then progressing with finer angular spacings. The reconstruction from the coarse steps is usually completed well before the acquisition of the fine-angle projection finishes. Therefore the user can view the reconstruction results from the coarsely spaced data when the projections of finer angular spacings are being acquired. This gives the user an opportunity to change parameters for preprocessing, reconstruction, and visualization, or to abort the acquisition. The acquisition sequence is currently controlled by the beamline operator with a program written in IDL (Interactive Data Language, Research Systems, Inc.). The other two stages of the tomography system, reconstruction and visualization, are performed by different routines written in C++ (more details in Section 3). Some manual synchronization is needed to initiate and maintain the pipeline. To make this system user-friendly enough for general users, an integrated graphical user interface (GUI) tool is being developed to control all three stages interactively in a straight-forward manner. In addition to attaching a GUI to the current acquisition program, this tool adds network functions that handle the data transfer and remote launching of the reconstruction and visualization calculations. Therefore the entire pipeline can be operated from the beamline experiment station.

3. COMPUTING STRUCTURE

The data files transferred from the acquistion system to the parallel computer store information on the experimental facility, the beamline, and the acquisition system in addition to the projetion data itself. They also contain information on the image processing routines to be applied to the projections and the reconstruction methods to be used along with the parameters for each operation. After the data files arrive at the parallel computer, they undergo several prelimary image processing steps such as normalization and alignment. The projections are then assembled into sinograms and reconstructed into volume slices. The reconstructed volume is then directed into another parallel

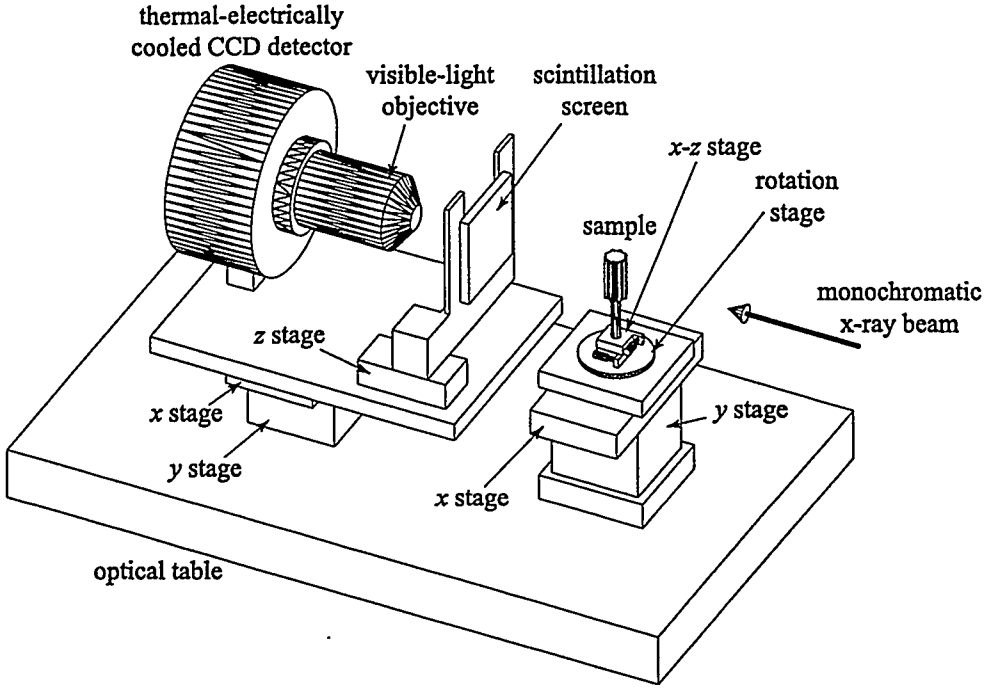

Figure 1. The straight-ray projection scheme used to acquire the tomographic projections. The x-ray beam is monochromatized by a Kohzu double-crystal monochromator. The monochromatic beam passes through the sample and reaches the $CdWO_4$ single-crystal scintillation screen. The visible light emitted by the scintillator is relayed to the CCD detector by a microscope objective. Both the sample and the detector are mounted on x-y stages for alignment to the x-ray beam. The sample is fixed on a minature x-z stage mounted on the rotation stage so that the sample's region of interest can be centered on the rotation axis. The scintillation screen is mounted on a z stage for visible-light objective focusing adjustment.

computer called the Viz Engine to interactively generate rendered images for viewing at video rate at both MCS and the APS experimental floor. Rendered still images are also periodically written to a web server to be viewed by collaborators world wide. This pipelined data acquisition and computation system is illustrated in Fig. 4.

3.1. Data File Structure

The data from the acquisition system are separated into a header file containing the experimental conditions and a series of data files that contain the actual projection data. The files are written in the Hierachical Data Format (HDF) created by the National Center for Supercomputing Applications.[8] The HDF format was chosen because of the following benefits:

- It is platform independent.
- It is self-describing.
- It supports nearly all data types that are likely to be used in experiments.
- It has a hierachical structure to organize a large number of data fields.

The content of the files is organized on the basis of the NeXus convention developed for the exchange of data from neutron- and synchrotron-based experiments.[9,10] The original NeXus data group definitions have been extended to accommodate the additional information required for tomography applications. The structure of the HDF header file is shown in Fig. 5. An API written in C++ was implemented to manage the data. The API has C++ class definitions that correspond to the HDF data structures.

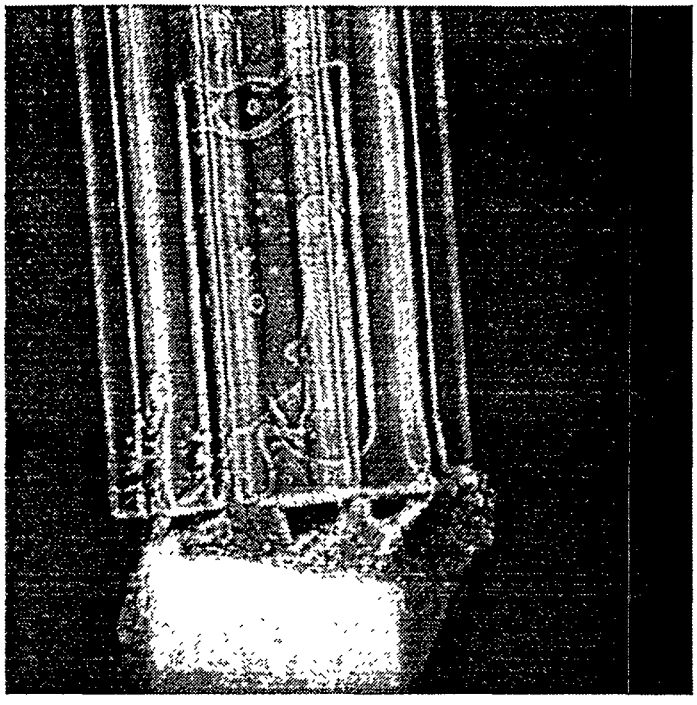

Figure 2. One projection of a micromachined gear acquired using 15 keV x rays using phase contrast. The gear was fabricated at the 2-BM beamline with the deep x-ray lithgraphy technique. It was made of PMMA with gold coating. The diameter of the gear is about 100 μm. The image consists of 512×512 pixels.

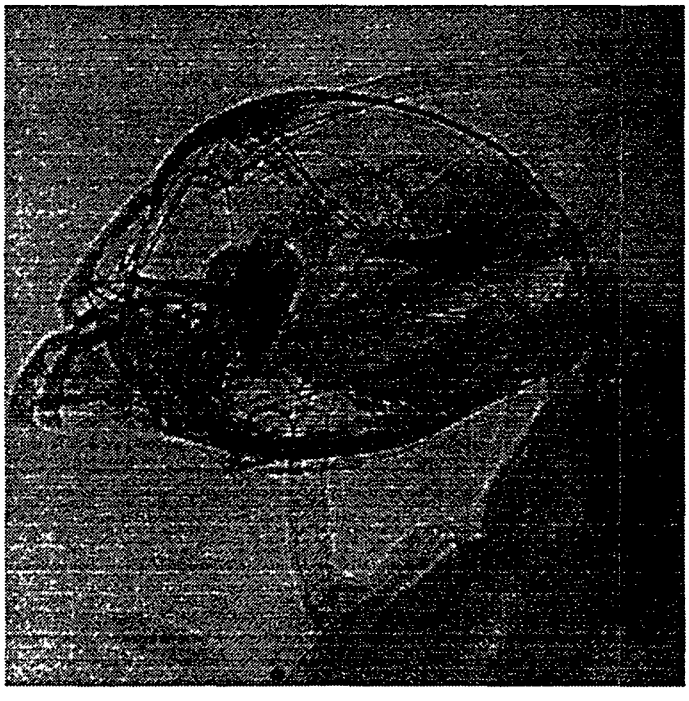

Figure 3. One projection of a carpenter ant's head acquired using 9 keV x rays in absorption-contrast mode. The field size was about 1.5 mm with 1024×1024 pixels.

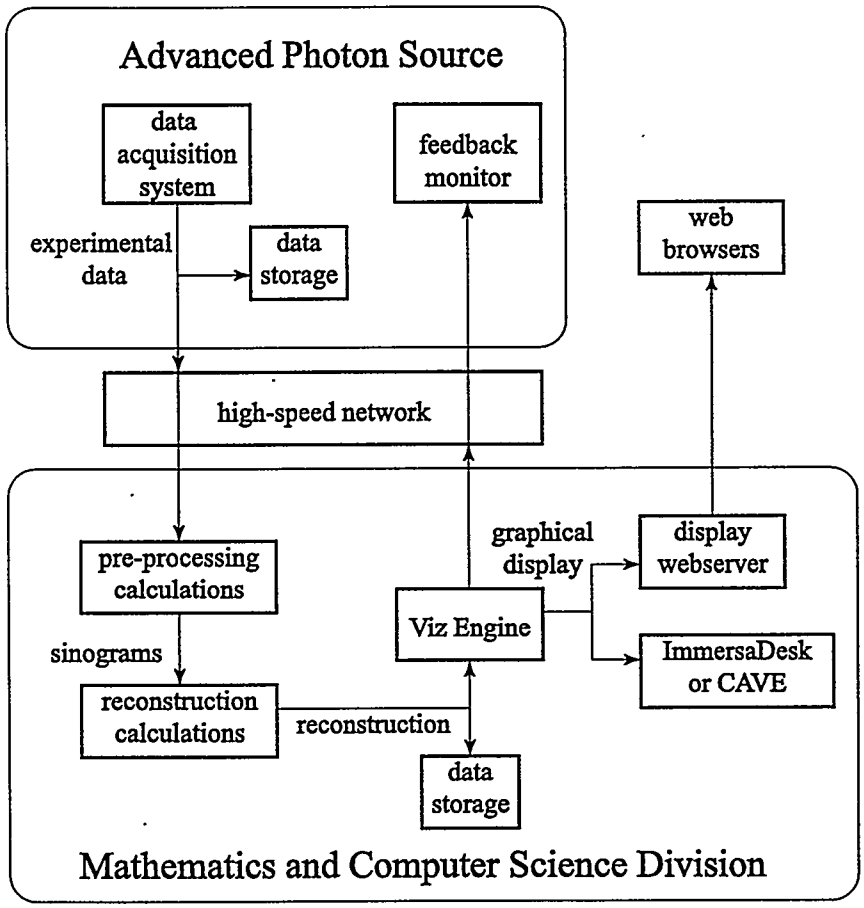

Figure 4. Illustration of the data acquisition and computation pipeline. An operator at the experiment station in the APS controls the data acquisition system and views the reconstruction result on the feedback monitor. The data acquired at the beamline is first written to a local hard disk and then transferred via a 100 Mb/second network to MCS. The preprocessing and reconstruction calculations are performed by the parallel computer. The reconstruction results are saved to a hard disk at MCS then fed into the Viz Engine. The Viz Engine provides rendered images interactively to the beamline feedback monitor via the high-speed network and also periodically writes rendered still images to a web server.

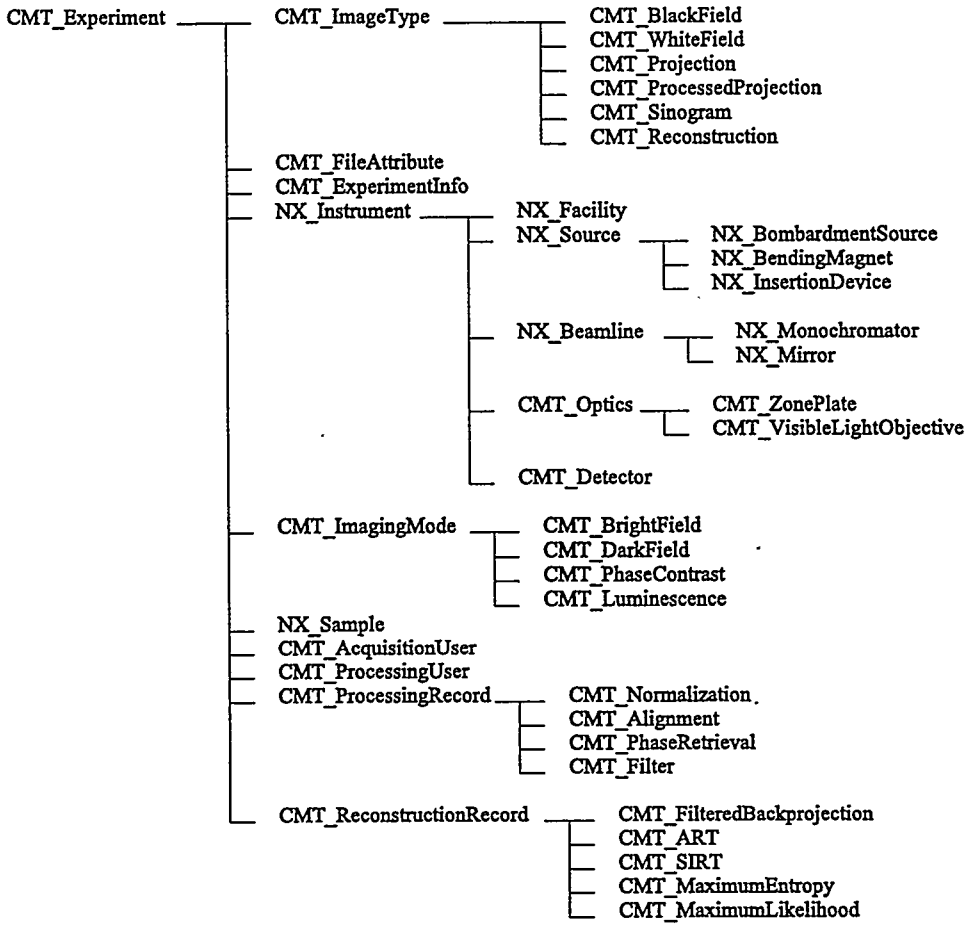

Figure 5. Group structure of the HDF header file and the class structure of the API written in C++. A time stamp and file version are stored in the CMT_FileAttribute. Information on the experiment operator and the experiment are stored in CMT_AcquisitionUser and CMT_ExperimentInfo groups. Experimental conditions, such as the facility, beamline, optics, detectors, and sample information are stored in NX_Instrument and NX_Sample. The imaging mode or contrast mechanism is stored in CMT_ImagingMode. Only one imaging mode is used for each header file. The header file also contains information on the type of images stored in the series of associated data files: for example, CMT_WhiteField and CMT_Projections are present in the raw data files while CMT_Sinogram is present in a series of files containing sinograms. The groups CMT_ProcessingUser, CMT_ProcessingRecord, CMT_ReconstructionRecord store information on the person performing the image processing and reconstruction along with the processing procedure and reconstruction methods used.

3.2. Parallel Computer System

A SGI Origin 2000 parallel computer with 128 nodes is used for the computations. It utilizes a grid-enabled computing environment with the Globus metacomputing toolkit.[11] Analogous to electric power grids, the Globus framework dynamically handles resource allocation, resource configuration, program submission, I/O operation, program scheduling, file staging, and uniform program executions within a system of processors or work stations.[12]

After the reconstructions are completed, the results are transferred to the Viz Engine for visualization calculations (see Fig. 4). The visualization software running on the Viz Engine software uses a hardware-optimized volume-rendering fuction library from Silicon Graphics called the Volumizer.[13] The rendered images can be viewed as a stereoscopic display on an ImmersaDesk in realtime at live video frame rates as the data volume is manipulated or as displayed parameters are changed. One limitation is that the data volume must have a size less than 256×256×256 pixels, hence our reconstructions often need to be subsampled before they can be loaded into the Viz Engine. The Viz Engine also periodically writes still images of the volume rendering to a web server so that the rendered displays can be viewed by collaborators worldwide. This feature is especially useful for experiments with a wide range of participation since, besides reducing the travel cost for the collaborators, it also allows a large number of specialists to provide prompt interpretation and feedback to the experiment operators.

3.3. Image Processing and Reconstruction

A number of image-processing operations are applied to the projection data before they are assembled into sinograms for reconstruction. An increasing collection of filters are being added to this preprocessing software package, and they can be selectively invoked by the user. The following are the currently implemented routines:

- *white field removal*: Removes the white field background of an image according to the Lambert-Beer law of x-ray absorption:

$$f' = \ln \frac{f_0}{f}, \tag{2}$$

  where f is the raw image, f_0 is the white field image and f' is the filtered image.

- *mean and median filter*: Replaces a pixel by a local average or median.

- *zinger filter*: Calculates the local mean (or median) and standard deviation at each image pixel. Replaces the pixel by the mean (or median) if the pixel value is more than a certain number of standard deviations away from the mean (or median).

- *Wiener filter (least square)*: Deconvolution using a predetermined point spread function weighed by the signal-to-noise spectrum.

The white field removal function is routinely used in the experiments to remove artifacts resulted from imperfections of the scintillation screen and beam non-uniformity. The mean/median and zinger filters are sometimes invoked to remove noise pixels from images. After the projections are filtered, they must be aligned so that they appear to rotate around a common axis. Two alignment algorithms are currently implemented:

- *centroid matching*: Shifts an image so that its centroid is located at a predetermined position.

- *cross-correlation*: Aligns two images to each other using the cross-correlation function.

Alignment using the cross-correlation method is more accurate and consistent but more time consuming and difficult to parallelize. For this reason, the centroid-matching method is often used in the live run while the cross-correlation method is mostly used in post-processing mode.

The reconstruction routines "ptomo" are based on code provided by Mark Ellisman and Steve Young from the National Center for Microscopy and Imaging Research at the San Diego Supercomputing Center.[14] Three commonly used algorithms are implemented: filtered backprojection, ART and SIRT. Because of the large number of projections acquired in our experiments, we have used filtered backprojection in our demonstrations and tests. Figures 6 and 7 show the screen captures from the visualization computer displaying the gear and ant data. They are of lower resolution than the reconstruction because of subsampling. A section of the ant-head reconstruction without the

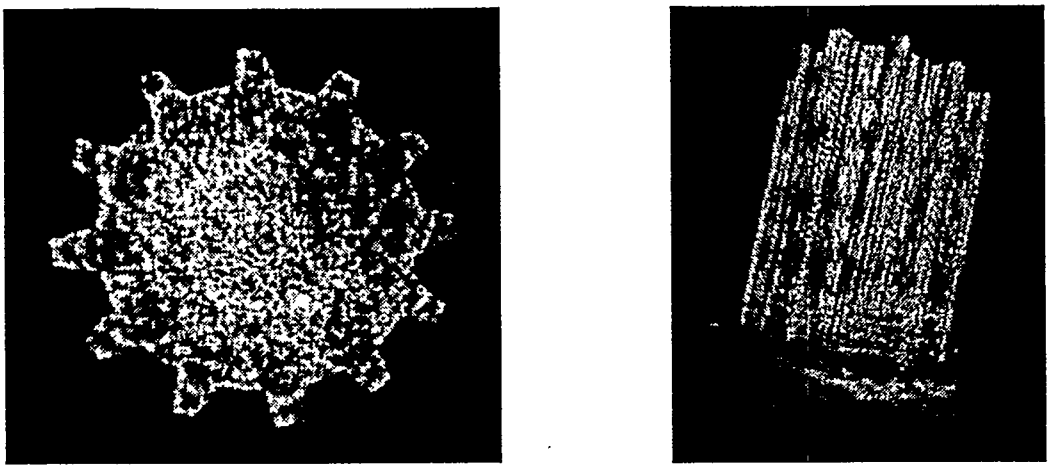

Figure 6. Reconstruction from the micromachined gear data. A section perpendicular to the gear axis is shown on the left, and a side view is shown on the right. (Screen captures, subsampled to 256×256×256.)

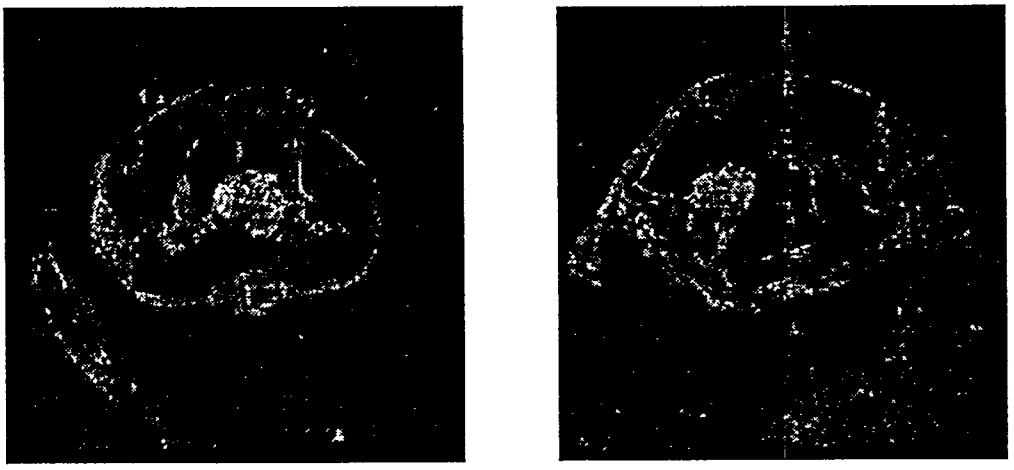

Figure 7. Sections of the reconstruction from the ant data. A "horizontal" section is shown at the left, and a "vertical" section is shown at the right. (Screen captures, subsampled to 256×256×256.)

subsampling is shown in Fig. 8. From our demo and test runs with 180 projections, each consisting of 512×512 16-bit integers and using 20 of the 128 processors, the preprocessing and reconstruction calculations can be completed in less than 10 min. When the data were acquired in a few cycles, the reconstruction from the starting cycles of typically only 12 to 24 projections can be viewed at the experiment station with 2 to 3 min.

4. DISCUSSION

This hard x-ray microtomography system has demonstrated quasi-realtime acquisition and reconstruction in the 10 min scale. Currently, the processes of data acquistion and computation take about the same amount of time, thus the two steps are "synchronized." We would like to reduce both time intervals so that the time requirement for the pipeline is only limited by the photon flux of the synchrotron. A number of changes have been planned to decrease the acquisition time to a few seconds:

- For our experiments in which only modest energy resolution is needed, the beamline efficiency can be improved by a factor of 10 by using a double-multilayer monochromator.

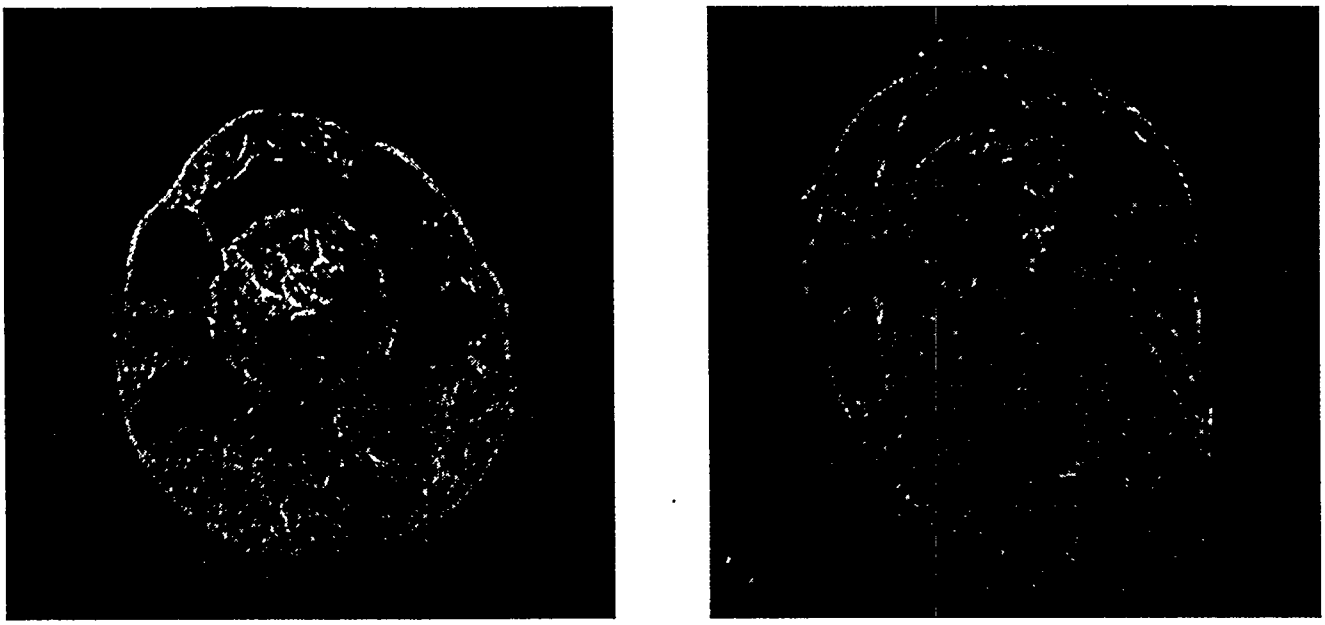

Figure 8. Two sections from the reconstruction using the ant data. The cavities of the cranium and the two incisors are clearly shown. The images consist of 512×512 pixels of 3 μm size.

- The detection system needs a scintillator that is better matched for 5-20 keV x-ray absorption.
- A high numerical aperture objective should be used.

These improvements can increase the combined efficiency of the beamline and the detection system by a factor of 100. Therefore the acquisition times can be reduced to the 10 s scale if the CCD readout time can be improved correspondingly. On the other hand, the computation time can also be reduced to under 1 min for 180 projections of 512×512-pixel images with the following improvements:

- Streamlining and parallelizing the preprocessing routines.
- Optimizing the reconstruction software from the San Diego Supercomputing Center for our computing platform acquisition scheme.

We are also planning to improve the spatial resolution of our tomography system on two fronts: a better scintillation screen and high numerical aperture objective can increase the resolution of our current setup to 1 μm, or, a PEEM based detection system has the potential of increasing the resolution to the 10 nm scale; an imaging type microscope is being developed at 2-ID-B (insertion device) beamline at the APS using 1-4 keV soft x rays and a zone plate optical element for magnification to produce 50 nm resolution. We are also making an effort to develop a graphical user interface system to control the acquisition, preprocessing, reconstruction, visualization steps so that this system can be used by general beamline users.

ACKNOWLEDGMENTS

This work is supported by the U.S. Department of Energy, Office of Basic Energy Sciences, Division of Material Sciences, under contract W-31-109-ENG-38.

REFERENCES

1. T. M. Breunig, J. C. Elliot, S. R. Stock, P. Anderson, G. R. Davis, and A. Guvenilir, "Quantitative characterization of damage in a composite material using x-ray tomographic microscopy," in *X-ray Microscopy III*, A. G. Michett and G. R. Morrison, eds., pp. 465–468, Springer-Verlag, Berlin, 1991.
2. J. H. Kinney, M. C. Nichols, U. Bonse, S. R. Stock, T. M. Breunig, A. Guvenilir, and R. A. Saroyan, "Nondestructive imaging of materials microstructures using x-ray tomographic microscopy," in *Materials Research Society Sym. Proc.*, Ackerman and W. A. Ellingson, eds., pp. 85–95, Materials Research Society, Pittsburg, 1990.
3. H.-R. Lee, B. Lai, W. Yun, D. C. Mancini, and Z. Cai, "X-ray microtomography as a fast three-dimensional imagin technology using a ccd camera coupled with a $cdwo_4$ single-crystal scintillator," in *SPIE Proc.*, vol. 3149, p. 257, Society of Photo-Optical Instrumentation Engineers (SPIE), (Bellingham, Washington), 1997.
4. W. S. Haddad, I. McNulty, J. E. Trebes, E. H. Anderson, R. A. Levesque, and L. Yang, "Ultra high resolution x-ray tomography," *Science* **266**, pp. 1213–1215, 1994.
5. J. Lehr, "3D x-ray microscopy: tomographic imaging of mineral sheaths of bacteria *Leptothrix ochracea* with the Göttingen x-ray microscope at BESSY," *Optik* **104**(4), pp. 166–170, 1997.
6. Y. Wang, C. Jacobsen, J. Maser, and A. Osanna, "Soft x-ray microscopy with a cryo stxm: Tomography," *Journal of Microscopy* , 1999, in press.
7. B. Lai, D. C. Mancini, W. Yun, and E. Gluskin, "Beamline and exposure station for deep x-ray lithography at the advanced photon source," in *SPIE Proc.*, vol. 2880, p. 171, Society of Photo-Optical Instrumentation Engineers (SPIE), (Bellingham, Washington), 1996.
8. *NCSA hdf homepage:* `http://hdf.ncsa.uiuc.edu/`.
9. P. Klosowski, M. Koennecke, J. Z. Tischler, and R. Osborn, "Nexus: A common format for the exchange of neutron and synchrotron data," *Physica* **B241-243**, pp. 151–153, 1998.
10. *NeXus homepage:* `http://www.neutron.anl.gov/NeXus`.
11. I. Foster and C. Kesselman, *The Grid: Blueprint for a New Computing Infrastructure*, Morgan Kaufman, 1998.
12. G. von Laszewski, J. A. Insley, I. Foster, J. Bresnahan, C. Kesselman, M.-H. Su, M. Thiebaux, M. L. Rivers, S. Wang, B. Tieman, and I. McNulty, "Real-time analysis, visualization and steering of microtomography experiment at photon sources," in *SuperComputing, Proc.*, vol. 217, p. 314, 1998.
13. R. Drebin, L. Carpenter, and P. Hanrahan, "Volume rendering," in *Proceedings of SIGGRAPH'88*, pp. 65–74, August, 1988.
14. P. J. Mercurio, T. T. Elvins, S. J. Young, P. S. Cohen, K. R. Fall, and M. H. Ellisman, "The distributed laboratory: An interative visualization environment for electron microscopy and three-dimensional imaging," *Comm. Assoc. Comp. Mach.* **35**, pp. 54–63, 1992.